Submolecular Structure and Orientation of Oligonucleotide Duplexes Tethered to Gold Electrodes Probed by Infrared Reflection Absorption Spectroscopy: Effect of the Electrode Potentials

SUPPORTING INFORMATION

László Kékedy-Nagy,[1] Elena E. Ferapontova,*[1] and Izabella Brand*[2]

[1] Interdisciplinary Nanoscience Center (iNANO) and Center for DNA Nanotechnology (CDNA), Science and Technology, Aarhus University, Gustav Wieds Vej 14, DK-8000 Aarhus-C, Denmark

[2] University of Oldenburg, Department of Chemistry, 26111 Oldenburg, Germany

* To whom correspondence should be addressed, I. Brand: izabella.brand@uni-oldenburg.de (phone: +49-441-798-3973, fax: +49-441-798-3979) or E. Ferapontova, elena.ferapontova@inano.au.dk (phone: +45-87156703, fax: +45-87154041)

S1. PM IRRA Spectra of the $(dAdT)_{25}$ /6-mercapto1-hexanol Monolayer on Au in the CH Stretching Modes Region

In the potential range -0.4 < *E* < 0.4 V vs. Ag/AgCl 6-mercapto1-hexanol molecules adsorbed on the gold electrode surface form stable monolayers. Potential cycling in this range does not affect the capacitance of the Au electrode covered by the $(dAdT)_{25}$-6-mercapto1-hexanol monolayer. Figure S3 shows the PM IRRA spectra of the $(dAdT)_{25}$-6-mercapto1-hexanol monolayer on gold in the CH stretching modes region. These spectra show four weak but well-resolved absorption bands centered at 2962 ± 2 cm^{-1}, a broad absorption mode around 2940 - 2930 cm^{-1}, and two absorption modes at 2904 ± 2 and 2850 ± 1 cm^{-1}. The high frequency mode is described to the $\nu_{as}(CH_3)$ mode of the methyl group of thymine. The corresponding $\nu_s(CH_3)$ mode expected around 2872 cm^{-1} is attenuated in the measured spectra, indicating an anisotropic orientation of the methyl groups of the dT base. The methylene bridge stretching modes arise from the 6-mercapto1-hexanol molecules. The $\nu_{as}(CH_2)$ mode is located at 2935-2930 cm^{-1} and from the high frequency side it overlaps with a Fermi resonance between the symmetric methyl stretching mode and the overtone of the symmetric methyl bending mode.[1] The low frequency side of the $\nu_{as}(CH_2)$ mode overlaps with the Fermi resonance between the symmetric – -CH_2- stretching mode and the overtone of the methylene bridge bending mode.[1] The $\nu_s(CH_2)$ mode is centered at 2850 cm^{-1}. Positions of the methylene bridge stretching modes indicate that the short hydrocarbon chains exist in a liquid phase.[1, 2] PM IRRA spectra in Figure S1 show that the -CH_2- groups give rise to very weak absorption modes. In addition, intensities of these modes are practically independent of the potential applied to the Au electrode (-0.4 V < *E* < 0.4 V vs. Ag|AgCl). Clearly, in the potential range of 6-mercapto1-hexanol adsorption on the Au surface, neither the surface concentration nor the orientation of the alkane chains in the chemisorbed molecules change.

This result is in excellent agreement with previous *in situ* spectroelectrochemical PM IRRAS studies of octadecanethiol molecules chemisorbed on the Au electrode surface.[3]

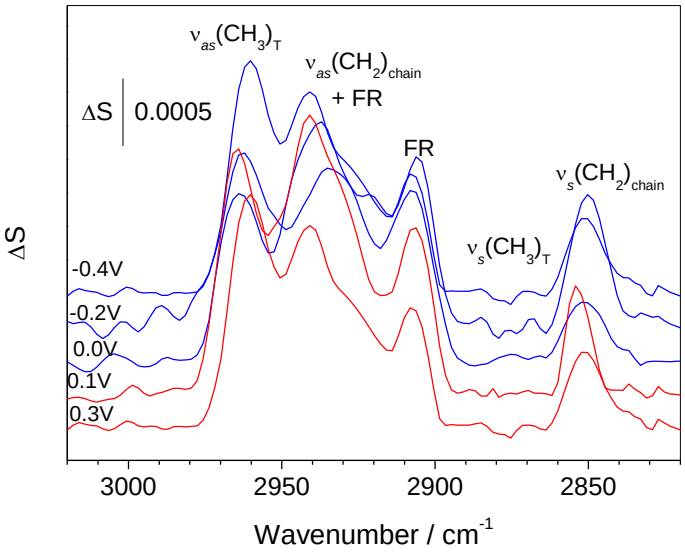

Figure S1. Representative PM IRRA spectra recorded in the CH stretching modes region of the $(dAdT)_{25}$-6-mercapto1-hexanol monolayer on the Au electrode surface at potentials marked in the figure. Blue lines represent spectra recorded at $E < E_{pzc}$ and red lines - at $E > E_{pzc}$.

S2. Isotropic Optical Constants of DNA Fragments

Experimental section: Transmission spectra of dsDNA containing either $(dAdT)_{25}$ or $(dGdC)_{20}$ base pairs (bp) were prepared by dissolving 40 µl of single stranded DNAs (ssDNA): 5'-AAA AAA AAA AAA AAA AAA AAA AAA A-3'(DNA-2); 5'-TTT TTT TTT TTT TTT TTT TTT T-3'(c-DNA-2); 5'-CCC GGG CCC GGG CCC GGG CC-3' (DNA-1) and 5'-GGG CCC GGG CCC GGG CCC GG-3' (c-DNA-1) (Metabion international, Planegg, Germany) in distilled water (D_2O or H_2O). Next, equal moles of two complementary ssDNA were mixed together and diluted in PBS (10 mM K_2HPO_4, 10 mM KH_2PO_4, 150 mM KCl and 100 mM $MgCl_2$) in either D_2O (Euroisotop, Saarland, Germany) or H_2O (18.2 MΩ, Type I, ELGA LabWater, Celle, Germany). All salts were purchased from

Aldrich, Steinheim, Germany. The total volume of the solution was equal to 200 µl. The mixture was left at room temperature for 75 minutes for hybridization. The final concentration of $(dAdT)_{25}$ duplexes was 3.8×10^{-4} M and that of $(dGdC)_{20}$ duplexes 5.3×10^{-4} M. The IR transmission spectra were measured using a flow cell (Aldrich, Steinheim, Germany) with a 25 µm thick Teflon spacer placed between two ZnSe optical windows. After the measurement of the background spectrum (buffer solution) the analyte spectrum was measured. The transmission IR spectra of $(dAdT)_{25}$ and $(dGdC)_{20}$ duplexes in D_2O were measured in 1800 – 1300 cm^{-1} spectral region providing the IR absorption bands of nucleic acid bp. Analogous experiments were performed in H_2O in order to measure IR spectra of DNA molecules in the 1300 – 1150 cm^{-1} spectral region (phosphate stretching modes). Isotropic optical constants: refractive index (*n*) and attenuation coefficient (*k*) were determined from transmission spectra as described in detail in previous publications.[4, 5] Isotropic optical constants of $(dAdT)_{25}$ and $(dGdC)_{20}$ duplexes are shown in Figures S2 and S3, respectively.

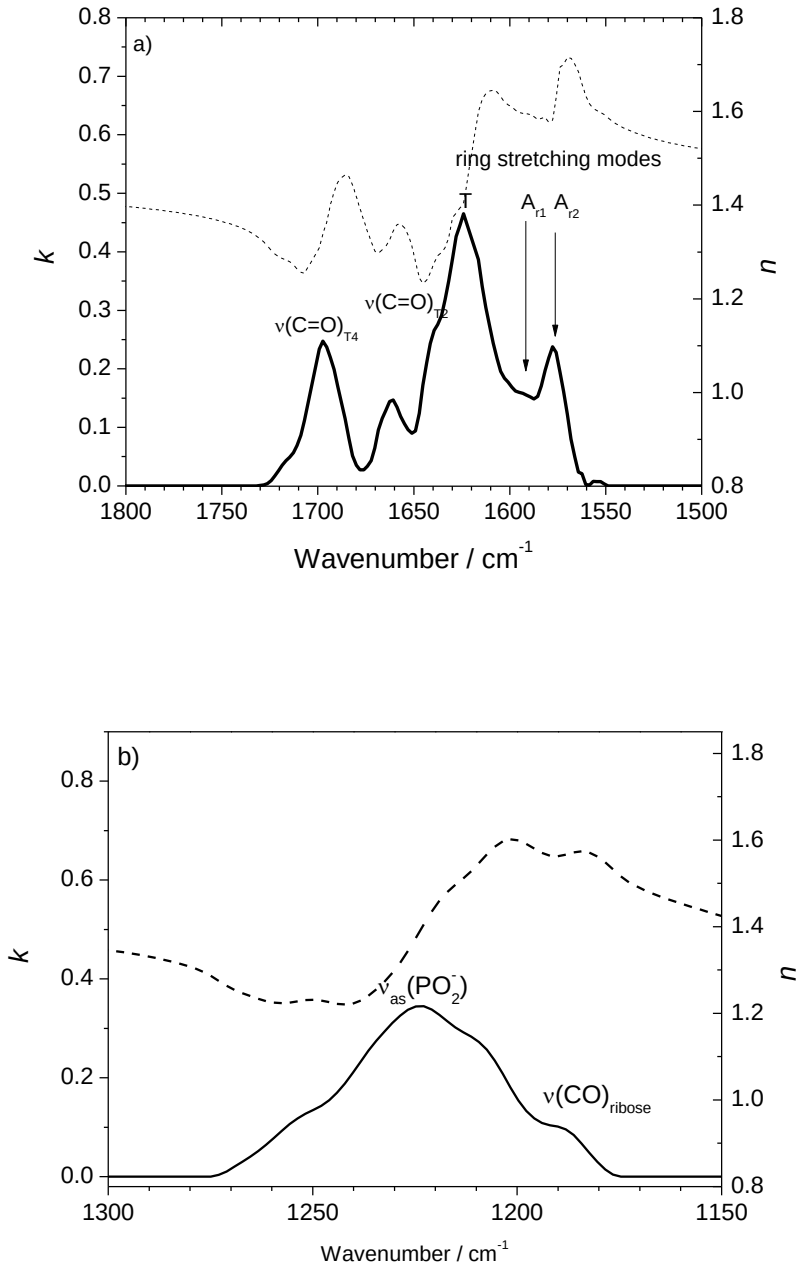

Figure S2. Isotropic optical constants of $(dAdT)_{25}$ duplexes: attenuation coefficient (*k*) and refractive index (*n*) in (a) 1800 – 1500 cm^{-1} and (b) 1320 – 1150 cm^{-1} spectral regions.

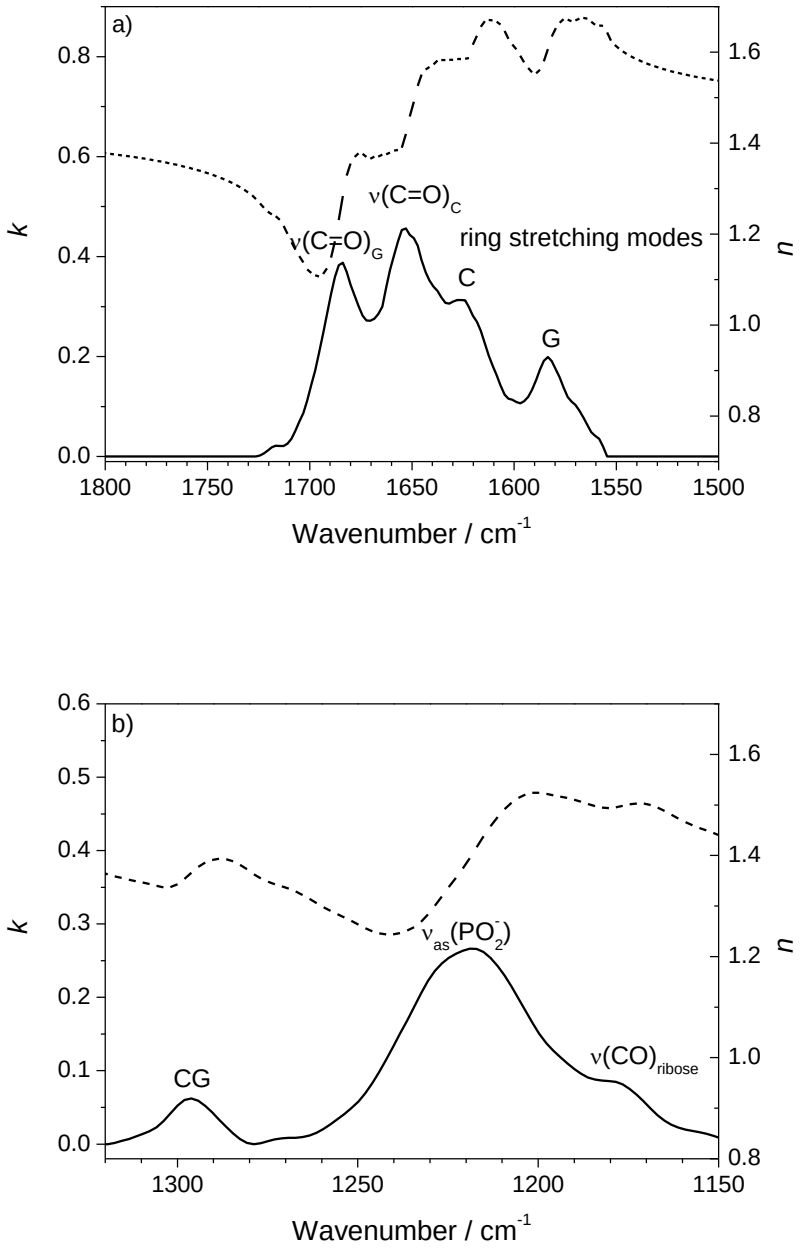

Figure S3. Isotropic optical constants of $(dGdC)_{20}$ duplexes: attenuation coefficient (k) and refractive index (n) in (a) 1800 – 1500 cm^{-1} and (b) 1320 – 1150 cm^{-1} spectral regions.

S3. In situ PM IRRA Spectra of dsDNA-6- mercapto1-hexanol Monolayers on the Au Surface

In situ PM IRRA spectra of $(dAdT)_{25}$-6-mercapto1-hexanol monolayers recorded in two independent experiments are shown in Figure S4. These spectra are compared with the spectrum of randomly distributed $(dAdT)_{25}$ molecules in a film corresponding to the thickness of a single molecule (8.5 nm, see the description below). Figure S4 shows that between independent experiments the maxima of absorption of different IR absorption modes originating from the nucleic acid bp in DNA molecules adsorbed on the Au surface differ by 0 – 4 cm^{-1}. Theoretical calculations of the IR absorption spectra of dsDNA fragments show clearly that in the D_2O solution the position of the deconvoluted IR absorption modes originating from a complementary bp depends on their hydration.[6-8] The corresponding shift of the IR absorption modes may be 30 cm^{-1} large. A small shift of the IR absorption modes observed in our experiments (0-4 cm^{-1}) suggests a slight variation of the degree of hydration of base pairs in different DNA monolayers adsorbed on the Au surface.

Quantitative analysis of the orientation of the planes of dA and dT bp requires knowledge of the intensities of the corresponding absorption modes for the random distribution of the studied molecules in the analyzed film.[5, 9] Figure S4 shows that the intensities of the analyzed IR absorption modes in the adsorbed monolayer are significantly attenuated. According to the surface selection rule of IRRAS [10], this result indicates that the transition dipole vectors of the C=O stretching modes in dT and the in-plane ring stretching modes in dA and dT adopt an almost parallel orientation. The ratio between the integral intensity of a given absorption mode measured by *in situ* PM IRRAS and analytically determined for the random orientation is a cosine function of the tilt angle of the transition dipole vector vs. the surface normal.[5, 11] PM IRRA spectra shown in Figure S4 show that at negative potentials the IR absorption mode at 1630 cm^{-1} is enhanced, whereas the intensity of the mode at ca. 1600 cm^{-1} is equal to zero.

At positive potentials, however, an opposite effect is observed. Despite low intensities of the measured spectra, their reproducibility is very good and indicates clearly that electrode potentials affect the shape and intensity of the PM IRRAS spectra and therefore the orientation of dsDNA in monolayer assemblies. Due to a large attenuation of the intensities of PM IRRA spectra in monolayer assemblies, the tilt angles determined in these two experiments differ only by 0 to 2 °.

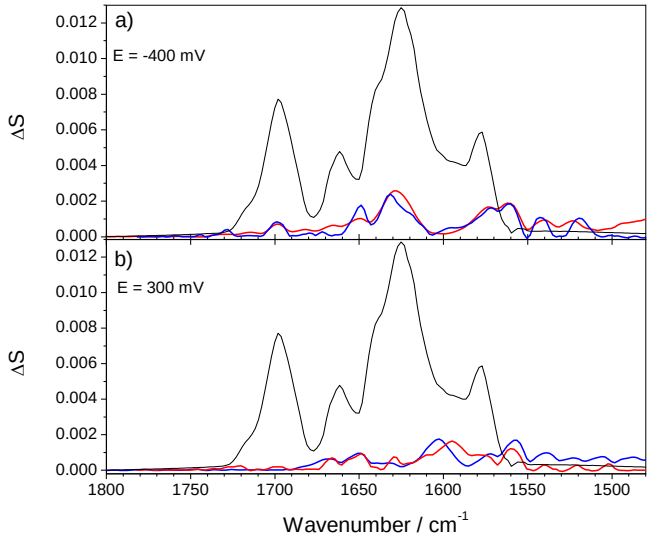

Figure S4. PM IRRA spectra in region 1800 – 1480 cm^{-1} of $(dAdT)_{25}$/6-mecrapto1-hexanol monolayer on Au measured in two independent experiments (blue and red line) overlapped with the spectrum of randomly distributed molecules in a 8.5 nm thick film (black line) at (a) E = -0.4 and (b) E = 0.3 V vs. Ag/AgCl.

S4. Calculation of PM IRRA Spectra of dsDNA Molecules Randomly Distributed in a Monolayer

Isotropic optical constants of $(dAdT)_{25}$ and $(dGdC)_{20}$ duplexes were used to calculate PM IRRA spectra of randomly distributed $(dAdT)_{25}$ and $(dGdC)_{20}$ molecules in a monolayer thick film following the procedure described earlier.[5, 12] In order to calculate these spectra the

thickness of the studied monolayer and the surface coverage (θ) of Au surface by DNA molecules in the monolayer have to be known.

X-ray diffraction data on DNA[13] were used to calculate the length of $(dAdT)_{25}$ and $(dGdC)_{20}$ molecules. Both DNA duplexes exist in aqueous solution in B-conformation. That is also valid for the monolayer assembly of $(dAdT)_{25}$, thus, for the calculation of the length of the $(dAdT)_{25}$ molecule (l) the axial rise of 0.34 nm [13] per bp was used. For the (dAdT) fragment composed of 25 bp the expected length of the duplex is l = 8.50 nm. In the case of $(dGdC)_{20}$ molecules, A- and B-DNA forms coexist in the monolayer formed on the gold electrode surface. Since the exact fraction of each form of $(dGdC)_{20}$ is unknown and in the solution phase only the B-form is found, the length of the $(dGdC)_{20}$ duplex was calculated in assumption of the B-form conformation. It is equal to l = 6.80 nm. Obviously, depending on the orientation of DNA molecules on the metal surface, the thickness of the DNA monolayer as well as the area available per molecule at the surface coverage equal to unity (θ_{max} = 1) change as schematically illustrated in figure S5.

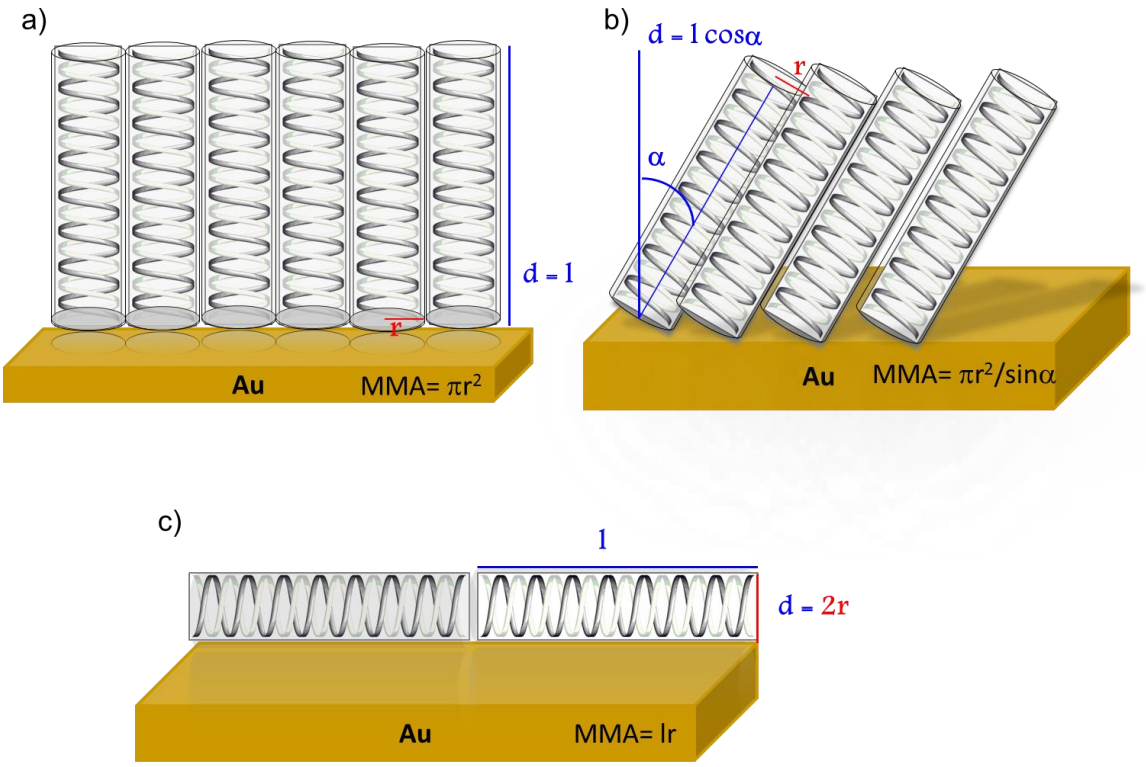

Figure S5. Schematic representation of the molecular packing of DNA molecules in monolayers on the Au electrode surface; a) vertical, b) tilted and c) parallel orientation of the long molecular axis with respect to the metal surface.

The shape of the dsDNA molecule is well approximated by a cylinder of the length *l* with the base radius *r*. The diameter of the B-from DNA double helix obtained in X-ray diffraction experiments is equal to 2.0 nm.[13] In the aqueous environment a thin layer of counterions surrounds the negatively charged helix,[14] resulting in an increase in the dimeter of the DNA molecule.[15-19] Reported values of the diameter of the DNA helix vary between 2.2 and 3.0 nm. Recent AFM studies show that the height of 2.74 ± 0.25 nm corresponds well to the dimeter of the DNA helix adsorbed on solid surfaces and immersed in aqueous electrolyte solution.[19] In this work, for the determination of the surface coverage of the Au electrode by the DNA molecules, the DNA diameter was set to 2.5 nm. Clearly, for the vertical orientation of a dsDNA molecule in the monolayer the film thickness (*d*) is equal to the length of the molecule (proportional to the number of bp), while the mean molecular area (MMA) is

determined by the surface of a circle with a radius r = 1.25 nm (Figure S5a). Tilting of the DNA molecules towards the metal surface results in the decrease in the monolayer thickness to $d = l \cos\alpha$, where α is the tilt of the helix vs. surface normal. Simultaneously, the MMA increases and is described by an elliptical footprint which is equal to $\pi r^2/\sin\alpha$ (Figure S5b).[16] Finally, in a film composed of DNA molecules oriented parallel to the metal surface, the monolayer thickness is equal to the diameter of the DNA molecule $d = 2r$ and the MMA is described by a rectangle with the area equal to $l \times r$ (Figure S5c).

Taking into account that dsDNA molecules tethered to a metal surface adopt a vertical or slightly tilted orientation with respect to the metal surface, the calculation of the PM IRRA spectrum of randomly distributed molecules in the monolayer was done considering the vertical orientation of macromolecules in the film (Figure S5a). Clearly, the film thickness is equal to the length of the dsDNA molecule ($d = l$). The MMA is equal then to the surface of a circle with r = 1.25 nm, giving MMA = 4.9 nm^2. For θ_{max} = 1 the maximal surface concentration of DNA molecules is $\Gamma_{DNA,max} = 2.04 \times 10^{13}$ molecules cm^{-2}. Electrochemical studies indicate that in our experiments the Γ_{DNA} of $(dAdT)_{25}$ and $(dGdC)_{20}$ duplexes in the monolayer on Au were 5.3 ± 0.1 and 5.6 ± 0.5 pmol cm^{-2}, respectively. These values correspond to the Γ_{DNA} of corresponding duplexes of $(3.19 \pm 0.06) \times 10^{12}$ and $(3.37 \pm 0.30) \times 10^{12}$ molecules cm^{-2}. These concentrations of the $(dAdT)_{25}$ and $(dGdC)_{20}$ molecules on Au give the average area occupied by a single duplex of 31.5 ± 0.73 nm^2 and 29.7 ± 2.5 nm^2, respectively. Thus, in the monolayer film of $(dAdT)_{25}$ duplexes the coverage (θ) of the Au surface by vertically oriented molecules is θ = 0.155 ± 0.004, and the coverage of the Au surface by the vertically oriented $(dGdC)_{20}$ duplexes is θ = 0.150 ± 0.03. The uncertainty in the determination of the surface coverage of the Au electrode by dsDNA molecules (the assumption of the diameter of the DNA molecule equal to 2.5 nm and the error of the determination of the surface concentration of $(dAdT)_{25}$ and $(dGdC)_{20}$ molecules in the

monolayer on Au) contributes to an error of 3 – 12 ° in the calculation of the tilt angle (ϕ) between transition dipole vectors of different IR absorption modes and the surface normal. The error in the determination of the tilt angle between independent measurements varies from 0 to 2°. Therefore, the error bars shown in this work include these two possible error sources. In these calculations, evaluated earlier isotropic optical constants were used. Moreover, the angle of incidence, thickness of the electrolyte layer and composition of the spectroelectrochemical cell (optical window: CaF_2, electrolyte: D_2O or H_2O, mirror: Au) were set to the same values as in the *in situ* PM IRRAS experiments.

S5. Deconvolution of the PM IRRA Spectra of dsDNA Molecules in Monolayer Assemblies

In order to perform deconvolution of the IR absorption modes, second derivatives of the experimental PM IRRA spectra of $(dAdT)_{25}$ and $(dGdC)_{20}$ molecules in monolayers formed on the Au surface were calculated. In the next step, the peak fitting procedure was used to calculate the integral intensity of the deconvoluted modes. The number and frequency of individual IR absorption modes contributing to the analyzed spectrum was set based on the second derivative and calculated frequencies of the IR absorption modes of the DNA fragments composed of either dAdT or dGdC bp.[6, 7] Figures S6 and S7 show the deconvoluted PM IRRA spectra in the "busy" spectral region of carbonyl and ring stretching modes of the $(dAdT)_{25}$ and $(dGdC)_{20}$ molecules in the monolayers formed on the Au surface.

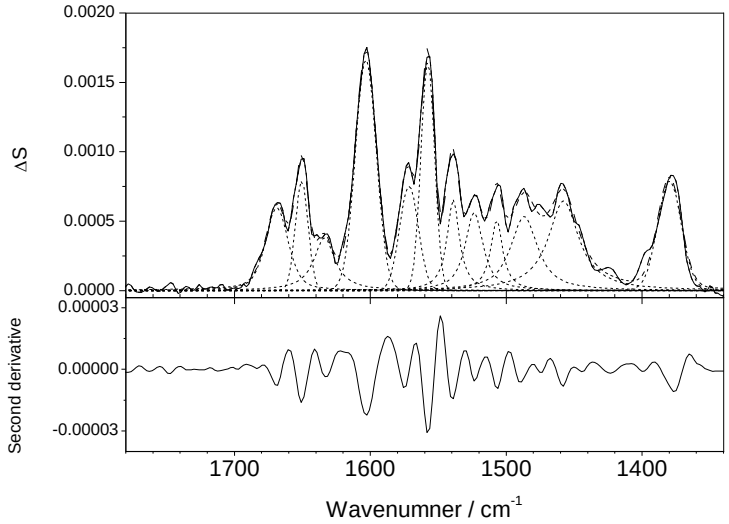

Figure S6. Upper panel: Experimental PM IRRA spectrum (thick line) and deconvoluted IR absorption modes originating from the $(dAdT)_{25}$ molecules in the monolayer on Au in the 1780 – 1340 cm^{-1} spectral region at E = 0.3 V vs. Ag/AgCl. Lower panel: second derivative of the PM IRRA spectrum.

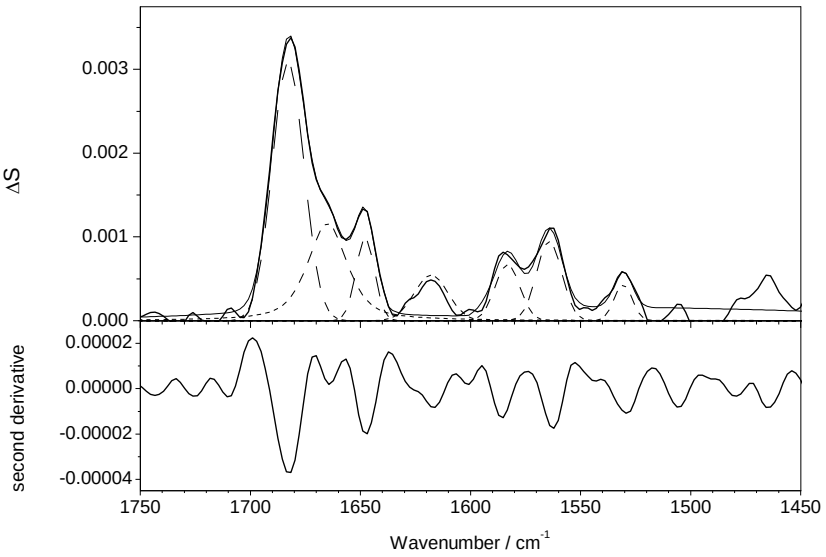

Figure S7. Upper panel: Experimental PM IRRA spectrum (thick line) and deconvoluted IR absorption modes originating from the $(dGdC)_{20}$ molecules in the monolayer on Au in the 1750 – 1450 cm^{-1} spectral region at E = 0.3 V vs. Ag/AgCl. Lower panel: second derivative of the PM IRRA spectrum.

References:

1. MacPhail, R. A.; Strauss, H. L.; Snyder, R. G.; Elliger, C. A. CH stretching modes and the structure of n-alkyl chains. 2. Long all-trans chains. *J. Phys. Chem.* **1984**, *88*, 334-341.
2. Snyder, R. G.; Strauss, H. L.; Elliger, C. A. C-H stretching modes and the structure of *n*-alkyl chains. 1. Long, disordered chains. *J. Phys. Chem.* **1982**, *86*, 5145-5150.
3. Anderson, M. R.; Gatin, M. Effect of applied potential upon the *in situ* structure of self - assembled monolayers on gold electrodes. *Langmuir* **1994**, *10*, 1638-1641.
4. Allara, D. L.; Baca, A.; Pryde, C. A. Distortions of band shapes in external reflection infrared spectra of thin polymer films on metal substrates. *Macromolecules* **1978**, *11*, 1215-1220.

5. Zamlynny, V.; Lipkowski, J. Quantitative SNIFTIRS and PM IRRAS of organic molecules at electrode surfaces. In *Adv. Electrochem. Sci. Eng.*, Alkire, R. C.; Kolb, D. M.; Lipkowski, J.; Ross, P. N., Eds. Wiley-VCH: Weinheim, 2006; Vol. 9, pp 315-376.

6. Lee, C.; Cho, M. Vibrational dynamics of DNA. II: Deuterium exchange effects and simulated IR absorption spectra. *J. Chem. Phys.* **2006,** *125*, 114509-1 - 114509-112.

7. Lee, C.; Cho, M. Vibrational dynamics of DNA: IV. Vibrational spectroscopic characteristics of A-, B-, and Z-from DNA's. *J. Chem. Phys.* **2007**, *126*, 14102-1 - 14102-10.

8. Lee, C.; Park, K. H.; Cho, M. Vibrational dynamics of DNA. I. Vibrational basis modes and couplings. *J. Chem. Phys.* **2006**, *125*, 114508-1 - 114508-16.

9. Kycia, A. H.; Su, Z. F.; Brosseau, C. L.; Lipkowski, J. In situ PM-IRRAS studies of biomimetic membranes supported at a gold electrode surface. In *Vibration spectroscopy at electrified interfaces*, Wieckowski, A.; Korzeniewski, C.; Braunschweig, B., Eds. Willey: Heidelberg, 2013; pp 345-417.

10. Moskovits, M. Surface selection rules. *J. Chem. Phys.* **1982**, *77*, 4408-4416.

11. Allara, D. L.; Nuzzo, R. G. Spontaneously organized molecular assemblies. 2. Quantitative infrared spectroscopic determination of equilibrium structures of solution - adsorbed n-alkanoic acids on an oxidized aluminum surface. *Langmuir* **1985**, *1*, 52-66.

12. Brand, I. Application of polarization modulation infrared reflection absorption spectroscopy under electrochemical control for structural studies of biomimetic assemblies. *Z. Phys. Chem.* **2016**, *230*, 133-183.

13. Wood, B. R. The importance of hydration and DNA conformation in interpreting infrared spectra of cells and tissues. *Chem. Soc. Rev.* **2016**, *45*, 1999-2018.

14. Manning, G. S. Counterion binding in polyelectrolyte theory. *Acc. Chem. Res.* **1979,** *12*, 443-449.

15. Kelley, S. O.; Barton, J. K.; Jackson, N. M.; McPherson, L. D.; Potter, A. B.; Spain, E. M.; Allen, M. J.; Hill, M. G. Orienting DNA helices on gold using applied electric fields. *Langmuir* **1998**, *14*, 6781-6784.

16. Hartwich, G.; Caruana, D. J.; de Lumley-Woodyear, T.; Wu, Y.; Campbell, C. N.; Heller, A. Electrochemical study of electron transport through thin DNA films. *J. Am. Chem. Soc.* **1999**, *121*, 10803-10812.

17. Levicky, R.; Herne, T. M.; Tarlov, M. J.; Satija, S. K. Using self-assembly to control the structure of DNA monolayers on gold: a neutron reflectivity study. *J. Am. Chem. Soc.* **1998**, *120*, 9787-9792.

18. Sam, M.; Boon, E. M.; Barton, J. K.; Hill, M. G.; Spain, E. M. Morphology of 15-mer duplexes tethered to Au(111) probed using scanning probe microscopy. *Langmuir* **2000**, *20*, 5727-5730.

19. Josephs, E. A.; Ye, T. A single-molecule view of conformational switching of DNA tethered to a gold electrode. *J. Am. Chem. Soc.* **2012**, *134*, 10021-10030.